Response by the authors:

Dear Andreas Lang (handling editor), dear anonymous referee,

we are very glad about the positive comments/evaluation of the referee and the following decision of you, Andreas Lang, which allows a publication of our submitted and revised article after further minor corrections.

We thank the referee for his/her helpful and constructive suggestions. We carefully addressed all of them and listed the changes done in the manuscript in detail hereafter.

Enclosed you find the revised main article with and without track changes.

Kind regards

Philipp Mamot

On behalf of all co-authors

RC = Referee comment

AR = Author response

RC: "p. 8, 2.1.1.: Is this one sentence necessary here? Could be figure text or the 1. Sentence of 2.1.2."

AR: We merged the sections 2.1.1 and 2.1.2 and shifted the two sentences of the old Sect. 2.1.1 to the beginning of the new section. The new title includes both old titles. The changed manuscript looks as follows (line 131):

"2.1 Characterisation of the mechanical and thermal setting

2.1.1 Model profile, rock joint geometry and kinematic analysis

The numerical model was set up in 2D and, thus, required a cross section of the summit crest. This profile covers a distance of 100 m, it runs from the north-face, across the crestline, to the south-face, and it crosses one of the main shear zones of the rockslide (Fig. 1a, Fig. 1b).

Four discontinuity sets (K1, K2, K3, K4) were identified in scan lines and field mapping (Fig. 3a). The profile for the mechanical model strikes at 146° which is in the direction of the assumed movement and follows the dip of the southern slope face (45/160). K2 (33/063) was excluded from the numerical analysis as the dip direction deviated by 66.5° from the model profile. The remaining joint sets deviating by 20–33° were implemented in the model as the standard deviations of their dip directions ranged between 5–20°, falling within the tolerable range of 30° deviation (Table 2). Joint set K1 represents the bedding planes and daylights in the south-face at an angle of 24° (Fig. 3b). .. "

Correspondingly, references to the subsections of 2.1 in the main text were adjusted, and in Fig. 1 the reference to the section for the "Joint set geometry" was changed from 2.1.2 to 2.1.1 (line 126, see below):

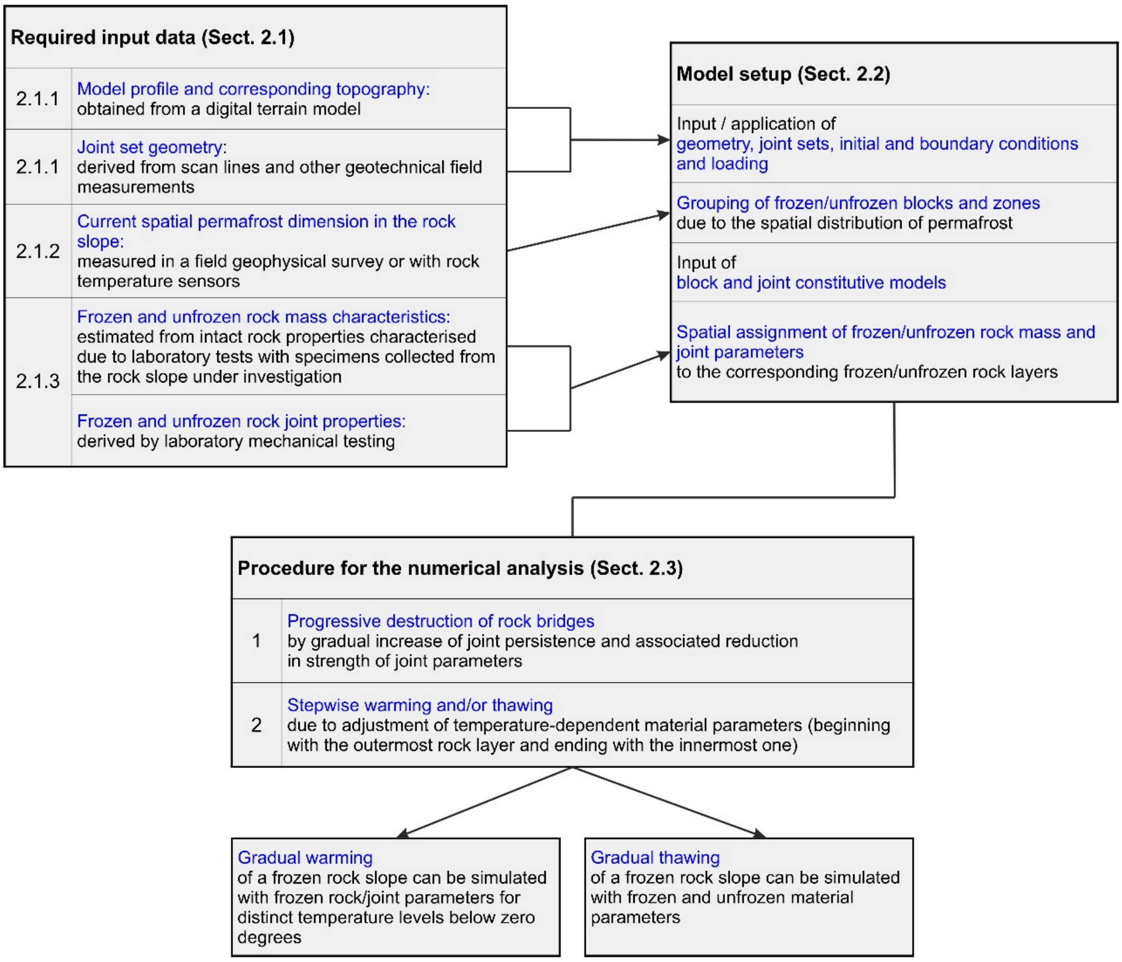

RC: "Discussion: Make sure that no results are duplicated there, focus on the discussion of the results, not the results itself. E.g. p. 32, chapter 5.3. starts very descriptive. Have a look with this in mind."

AR: As suggested by the referee, we revised the first paragraphs of Sections 5.2 and 5.3 in the following way:

Line 585:

"5.2 Stability assessment of the warming/thawing Zugspitze summit crest based on the factor of safety

The numerical model for the Zugspitze summit ridge simulates the strength reduction at warming and thawing based on laboratory tests of this and of previous studies (Table 1). Warming of ice-filled joints takes the slope close to a critical level of stability (FS = 1.3), but it does not initiate instability. As soon as thawing sets in and the ice is lost, the south-face becomes massively destabilised as displacements increase by two orders of magnitude and *the factor of safety falls below unity. The reduction in joint stability is significantly influenced by a loss of the joint cohesion from 0.18 MPa (at -0.5 °C) to 0 MPa (Table 5), even though the joint friction angle is increased from 13.5 to 29.3°. In contrast to our numerical analysis, Davies et al. (2001) postulate that the FS of a permafrost affected rock slope is higher for unfrozen joints than for ice-filled joints between approximately -1.5 °C and zero degrees. The differing observations on the stability upon thaw may be explained as follows: …"*

[…]

Line 627:

5.3 The stability of a simplified permafrost rock slope with rising temperature

A permafrost rock slope with ice-filled joints and a fracture network and rock/joint properties similar to the Zugspitze south-face can become unstable at a slope gradient > 50 or 55° (transition from Domain 1 to Domain 2 in Fig. 8). This range of inclinations seems to be the most critical in terms of slope destabilisation, as it is characterised by the highest relative increase in displacements per degree of the slope angle. Interestingly, this could be confirmed by the study of the critical slope angle for varying orientations of the fracture network (Fig. 9): 50 % of the studied orientations have a critical slope angle of 50 or 55°, which corresponds to the transition from Domain 1 to Domain 2. 30 % of the orientations lead to instability with angles of between 57.5–62°, and 20 % remain stable within the studied range of slope gradients. .."

RC: "Conclusions: many points, consider to merge some of them. I find the passage from l. 710 much a discussion again. Maybe stop after the first sentence as a final remark, all other stuff is could be deleted or mentioned in the discussion."

AR: As proposed by the referee, we merged some of the listed points in the conclusions which looks as follows (line 684):

"[…] The related main findings are summarised as follows:

- *(i)* *The proposed instruction for the temperature-dependent mechanical stability model can be used for any permafrost-affected rock slope across the globe which is subjected to climatic warming.*
- *(ii)* *Laboratory tests and field reconnaissance of the benchmark site Zugspitze exemplify thermal, geometrical and mechanical input data for the numerical model. Frozen and unfrozen bedrock material properties were assigned to specific sections in the model and changed due to warming/thawing. The modelling procedure was divided into three stages: rock bridge destruction, warming with ice-filled joints, and thawing. Process-specific and temperature-dependent input parameters were modified when switching from one stage to the next.*
- *(iii)* *The Zugspitze model demonstrates a stability decrease towards a critical level as a result of (a) rock bridge destruction and (b) gradual warming of frozen rock and ice-filled joints from -4 to -0.5 °C. Surficial rock slope failure starts coincident to thawing of the outermost rock layer. Upon full thaw of the summit crest, expected within the next five decades, the model predicts an increase in displacements which potentially lead to final slope failure.*

(iv) We developed a framework to generalise and upscale the Zugspitze model. A sensitivity analysis with simplified geometry and warming pattern was performed to calculate the following critical stability thresholds: (a) The dependence between instability and the slope angle can be classified into a stable first domain (≤ 50°), a second domain with a first onset of instability (55–62°), and a third domain characterised by an accelerated slope destabilisation (≥ 64°). The greatest relative increase in displacements is observed in the second domain. (b) Warming from -4 °C to a temperature between -3 and -0.5 °C initiates instability for rock slopes ≥ 50°. Destabilisation is more pronounced for warming closer to the melting point (from -2 to -0.5 °C) than for warming from -4 to -2 °C. This difference becomes greatest in the second domain. (c) For anaclinal slopes, the critical slope angles range between 50–62°, and for cataclinal slopes, they range between 55–62°.

(v) The calculated critical slope angles and rock mass temperatures correspond well to the characteristics of documented rock slope failures in permafrost areas in the European Alps, which often showed large amounts of residual ice in their scars.

(vi) The critical thresholds can be applied to warming permafrost rock slopes with (a) ice-filled joints, (b) limestone equivalent to Wetterstein limestone, or probably most of the rock types relevant for permafrost rock slope failure in the Alps, (c) slope angles smaller than 70° and (d) various orientations of the fracture network consisting of three joint sets.

(vii) The critical thresholds can be used to detect rock slopes which are susceptible to fail in the future and potentially endanger human life and mountain infrastructure. For this, it is a prerequisite to have data on the fracture network, lithology, geometry and the thermal field of the investigated rock slopes. In contrast, a detailed stability assessment of a single rock slope requires a number of further site-specific input data.

[…]..”

The last paragraph was fully shifted to the end of Section 5.1 – Limitations (line 565):

“- *Warming to the next degree centigrade was, by default, calculated with 3000 cycles which was a compromise between a representative number of cycles for potentially reaching a numerical equilibrium (for stable rock slopes), and a reasonable, not too time-consuming calculation. Computations for low/intermediate slope angles and temperatures reached an equilibrium prior to 3000 cycles, while calculations for higher slope angles and temperatures mostly failed to reach an equilibrium (for unstable rock slopes) or scarcely required > 3000 cycles. Hence, the numerical calculation was repeated with warming steps with 6000 cycles to test a potential cut-off effect of cycles required for the rock slope to react to a change in stress-strain due to a modification of material parameters. However, the results coincide well with the model runs with 3000 cycles since displacements significantly accelerate above slope angles of 50° and 62°, and they are higher for temperatures closer to melting (Fig. S8).*

We are at the beginning of developing numerical models for the mechanical response of a rock mass to warming/thawing. Therefore, there is a huge potential for improvements. For instance, more mechanical laboratory tests are necessary to improve process understanding and to extend the number of frozen and unfrozen material parameters for modelling. Future numerical models should be based on further sensitivity analyses, or include water pressure or the creep of ice at lower displacement rates within the advanced stage of rock slope destabilisation. Time-dependent cycling is not yet implemented in most of the numerical models, neither it is in the presented ones. Hence, they are not suited to forecast a precise time of rock slope failure. Further, the spatial warming pattern for the Zugspitze model is simplified and based on *a static temperature field derived from ERT, rock thermistors and published thermal models. For a more accurate characterisation of the warming pattern, future mechanical models should include a subsurface temperature field based on a combination of geophysics and a heat flow model for different time steps."*

[…]

RC: "References: This paper was in revision a very long time, make a last check that all relevant new literature is cited (little/0? references after 2017). Maybe there are none, but do a thorough check before publishing."

AR: We added the following new references to the main text (highlighted in red colour):

- Line 39: "*Some prominent examples are the 2003 Matterhorn block fall (0.002 Mio m³; Weber et al., 2019), the 2014 Piz Kesch rock slope failure (0.15 Mio m³; Phillips et al., 2017) and the 2017 Pizzo Cengalo failure with 8 fatalities (3–4 Mio m³; Walter et al., 2020; Mergili et al., 2020) in Switzerland, the 1987 Val Pola debris avalanche in the Italian Alps (33 Mio m³; Dramis et al., 1995), the 2005 Mt. Steller rock-ice avalanche in Alaska (40–60 Mio m³; Huggel et al., 2010) and the 2002 Kolka/Karmadon rock-ice avalanche with 140 fatalities in the Russian Caucasus (100 Mio m³; Huggel et al., 2005)."*
- Line 50: "..*The ductile temperature- and stress-dependent creep of ice and ice-rich soils has been investigated by e.g. Arenson and Springman (2005), Bray (2013) and Sanderson (1988)."*
- Line 54: "*The mechanics of frozen and unfrozen intact rock have been studied by e.g. Dwivedi et al. (2000), Inada and Yokota (1984), Kodama et al. (2013), Mellor (1973), Pläsken et al. (2020) and Voigtländer et al. (2014)."*
- Line 188: "*This technique has been used to characterise and monitor the spatial variability and evolution of mountain bedrock permafrost in steep rock walls (Keuschnig et al., 2017; Krautblatter et al., 2010; Magnin et al., 2015; Murton et al., 2016; Scandroglio et al., 2021)."*
- Line 265: *"Values for the elastic rock mass shear and bulk moduli Gm and Km were derived according to the equations presented by Tipler and Mosca (2015) for intact rock:…"*
- Line 289: **"Table 1: Laboratory-tested strength reduction of intact dolomised Wetterstein limestone due to thawing. Standard deviations (indicated with ±) are given for measured parameters, and they were used for determination of minimum and maximum values (given in parentheses) of the calculated parameters. RMC refers to parameters that are used for rock mass characterisation.**

Mechanical parameter	Saturated frozen (-5 °C)	Saturated unfrozen (+22 °C)	Decrease due to thawing %	% °C⁻¹	Test / equation applied	RMC
Density ρ [g/cm³]	--	2.7 ± 0.01	--	--	Weighing tests in water bath	x
Porosity n [%]	--	0.9 ± 0.4	--	--	Weighing tests in water bath	
Shear modulus G [GPa]	32.4 (31.7/32.6)	25.8 (21.9/29.2)	20.4	0.8	Eq. (2), after Tipler and Mosca (2015)	
Bulk modulus K [GPa]	70.3 (64.8/74.8)	55.9 (40.4/76.0)	20.5	0.8	Eq. (3), after Tipler and Mosca (2015)	
Young's modulus E [GPa]	84.3 (81.7/85.3)	67.1 (55.7/77.6)	20.4	0.8	Eq. (4), after Tipler and Mosca (2015)	
Poisson's ratio υ	0.3 ± 0.01	0.3 ± 0.03	0	0	Ultrasonic tests	x
Dilatational wave velocity V_D [m/s]	5560 ± 50	4950 ± 400	11.0	0.4	Ultrasonic tests	

Uniaxial tensile strength σ_t [MPa]	9.0 ± 1.4	7.2 ± 1.9	20.0	0.7	Brazilian tests	
Uniaxial compressive strength σ_c [MPa]	109 ± 25	91 ± 27	16.5	0.6	Uniaxial compressive strength tests	x

- Line 293: **Table 2: Estimated and calculated strength reduction of Wetterstein limestone rock mass due to thawing, derived from the GSI scheme after Hoek and Brown (1997). Minimum and maximum values of calculated parameters are given in parentheses. These were determined with the standard deviations of the measured parameters (Table 3). IP = used as input parameter for the numerical model.**

Mechanical parameter	Saturated frozen (-5 °C)	Saturated unfrozen (+22 °C)	Decrease due to thawing %	% °C^{-1}	Test / equation applied	IP
Young's modulus E_m [GPa]	24.8 (21.7/27.5)	22.6 (19.0/25.8)	8.9	0.3	Eq. (1), after Hoek et al. (2002)	
Shear modulus G_m [GPa]	9.5 (8.4/10.5)	8.7 (7.5/9.7)	8.4	0.3	Eq. (2), after Tipler and Mosca (2015)	x
Bulk modulus K_m [GPa]	20.6 (17.2/24.1)	18.9 (13.7/25.3)	8.3	0.3	Eq. (3), after Tipler and Mosca (2015)	x
Uniaxial tensile strength σ_{tm} [MPa]	-0.9 (0.7/-1.1)	-0.7 (-0.5/-0.9)	22.2	0.8	Eq. (5), after Hoek et al. (2002)	x
Friction angle φ_m [°]	44[a]	44	0	0	estimated after Cai et al. (2004)	x
Cohesion c_m [MPa]	3.9	3.3	15.4	0.6	estimated after Cai et al. (2004)	x
Parameter of the Hoek-Brown strength criterion						
GSI value	--	65	--	--	estimated after Marinos and Hoek (2000)	
m_i	--	9	--	--	estimated after Marinos and Hoek (2000)	
m_b	--	2.6	--	--	calculated after Hoek et al. (2002)	
s	--	0.02	--	--	calculated after Hoek et al. (2002)	
Disturbance factor D	--	0	--	--	estimated after Hoek et al. (2002)	

Note: [a]The frozen rock mass friction angle was given the same value as for the unfrozen friction angle, resulting in a decrease in thawing of zero.

- Line 332: "*Similarly, the measured unfrozen φb corresponds well to the values listed e.g. in Barton and Choubey (1977) or Ulusay and Karakul (2016).*"

The citations have been included in the references at the end of the manuscript.